HHS Public Access

Author manuscript

Sci Transl Med. Author manuscript; available in PMC 2022 May 23.

Published in final edited form as:

Sci Transl Med. 2021 October 20; 13(616): eabe2352. doi:10.1126/scitranslmed.abe2352.

A rapid assay provides on-site quantification of tetrahydrocannabinol in oral fluid

Hojeong Yu[1,2,3], **Hoyeon Lee**[4], **Jiyong Cheong**[3,5], **Sang Won Woo**[6], **Juhyun Oh**[1,2], **Hyun-Kyung Oh**[4], **Jae-Hyun Lee**[3,5], **Hui Zheng**[7], **Cesar M. Castro**[1,8], **Yeong-Eun Yoo**[6], **Min-Gon Kim**[4], **Jinwoo Cheon**[3,5,9], **Ralph Weissleder**[1,2,10], **Hakho Lee**[1,2,*]

[1.]Center for Systems Biology, Massachusetts General Hospital Research Institute, Boston, MA 02114, USA.

[2.]Department of Radiology, Massachusetts General Hospital, Harvard Medical School, Boston, MA 02114, USA.

[3.]Center for Nanomedicine, Institute for Basic Science (IBS), Seoul 03722, South Korea.

[4.]Department of Chemistry, School of Physics and Chemistry, Gwangju Institute of Science and Technology, Gwangju 61005, South Korea.

[5.]Graduate Program of Nano Biomedical Engineering (NanoBME), Advanced Science Institute, Yonsei University, Seoul 03722, South Korea.

[6.]Department of Nano Manufacturing Technology, Korea Institute of Machinery and Materials, Daejeon 34103, South Korea.

[7.]Biostatistics Center, Massachusetts General Hospital, Boston, MA 02114, USA.

[8.]Department of Medicine, Massachusetts General Hospital, Boston, MA 02114, USA.

[9.]Department of Chemistry, Yonsei University, Seoul 03722, South Korea.

[10.]Department of Systems Biology, Harvard Medical School, Boston, MA 02115, USA.

Abstract

Tetrahydrocannabinol (THC), the primary psychoactive ingredient of cannabis, impairs cognitive and motor function in a concentration-dependent fashion. Drug testing is commonly performed for employment and law enforcement purposes; however, available tests produce low-sensitive binary results (lateral flow assays) or have long turnaround (gas chromatography-mass spectrometry). To enable on-site THC quantification in minutes, we developed a rapid assay for oral THC analysis called EPOCH, ***e***xpress ***p***robe for ***o***n-site ***c***annabis in***h***alation. EPOCH features distinctive sensor

[*]Corresponding author: H. Lee, PhD, Center for Systems Biology, Massachusetts General Hospital Research Institute, 185 Cambridge St, CPZN 5206, Boston, MA, 02114, USA, 617-726-6487, hlee@mgh.harvard.edu.

Author contributions: H.Y., M.-G.K., C.M.C., Jinwoo C., R.W., and Hakho L. designed the study. H.Y. developed EPOCH assay. H.Y., Hoyeon L., J.O., and H.-K.O. performed material characterization. H.Y. developed the software and algorithms. H.Y., S.W.W., and Y.-E.Y. devised and manufactured the kit with instrument. Hoyeon L. characterized the binding kinetics. Hoyeon L., Jiyong C. and J.-H.L. evaluated gold nanoparticle complexes. H.Y., H.Z., and Hakho L. conducted EPOCH experiments and analyzed the data. H.Y. and Hakho L. prepared figures, and H.Y., R.W., and Hakho L. wrote the manuscript with the help of all authors.

Competing interests: R.W. declares that he has received consultancy payments from Accure Health, and that he is a shareholder of Lumicell. Hakho L. declares that he has received consultancy payments from Accure Health.

design such as a radial membrane and transmission optics, all contained in a compact cartridge. This integrated approach permitted assay completion within 5 minutes with a detection limit of 0.17 ng/mL THC, which is below the regulatory guideline (1 ng/mL). As a proof of concept for field testing, we applied EPOCH to assess oral fluid samples from cannabis users (n = 43) and controls (n = 43). EPOCH detected oral THC in all specimens from cannabis smokers (median concentration, 478 ng/mL) and THC-infused food consumers. Longitudinal monitoring showed a fast drop in THC concentrations within the first 6 hours of cannabis smoking (half-life, 1.4 hours).

One Sentence Summary:

The ***e***xpress ***p***robe for ***o***n-site ***c***annabis in***h***alation (EPOCH) system is able to quantitates tetrahydrocannabinol concentrations in oral fluid.

Introduction

Cannabis is a commonly utilized psychoactive drug, with an estimated 180 million users worldwide. In the United States (US), more than 43 million people use cannabis (1), and the proportion of daily or near-daily users (>40%) is rising due to the legalization of cannabis for recreational and medicinal use. Although recognized for its therapeutic and recreational benefits (2, 3), cannabis also raises public health concerns regarding users operating machinery or driving under its influence. When inhaled through smoking or vaping, the primary psychoactive ingredient of cannabis, Δ^9-tetrahydrocannabinol (THC), rapidly enters circulation and reaches the brain. Acute psychological effects set in within minutes and last for two to four hours (4, 5). Driving motor vehicles during this period should be avoided, as cognitive functions (for example, decision making and concentration) and motor functions (for example, reaction time and coordination) are compromised (6–8). In controlled road tests, drivers under the influence of cannabis exhibited impaired vehicle control (8–10); several epidemiology studies found that cannabis users are at higher risk for accidents (11–13). As such, an unmet need remains for rapid, accurate, and on-site THC detection motivated by scenarios entailing public health safety.

Several currently available analytical tests can detect THC in human bodily fluids. The gold standard, gas chromatography-mass spectrometry (GC-MS) of blood and urine samples, is generally performed in specialized laboratories and could take days to process (14, 15). Test results could also be ambiguous in determining the last time of cannabis consumption (16, 17). Residual THC and its metabolites are often present in bodies weeks after cannabis intake, and it is challenging to separate acute recent from chronic use (17–20). Conversely, high THC concentrations in oral fluid have been shown to directly correlate with immediate (<12 hours) cannabis use (21–23). Monitoring oral THC concentrations can thus enable a range of safety applications: precautionary self-monitoring by cannabis users, roadside testing by law enforcement, and drug screening in the public sector. Unfortunately, existing commercial test kits have suboptimal analytical capacities including low sensitivity and binary results, and laboratory-based tests require sophisticated instrumentation (see Table S1), a drawback to routine, on-site THC detection (24–26).

Here, we describe the development of a quantitative, dynamic oral fluid test, EPOCH (***e***xpress ***p***robe for ***o***n-site ***c***annabis in***h***alation), capable of measuring THC concentrations within 5 minutes. EPOCH quantitates oral THC concentrations down to 0.17 ng/mL, which is below the recommended regulatory cutoff of 1 ng/mL (the European Driving under the Influence of Drug, Alcohol, and Medicines; DRUID) and similar to results from GC-MS analyses (27). Our method integrates several key engineering advances: i) a radial-membrane flow strategy to enhance sensor kinetics, boosting both sensitivity and speed; ii) a modular, injection-molded cartridge streamlining reliable, high-precision sample processing for THC quantification; and iii) an optical sensing mechanism of transmission that detects higher analytical signals than the conventional reflection mode. The EPOCH test is unaffected by the consumption of coffee, alcohol, or tobacco and other confounding factors. When applied to oral fluid samples from cannabis users (n = 43) and controls (n = 43), EPOCH showed excellent detection accuracy. Our results also show that THC concentrations fell below the DRUID guideline (1 ng/mL) within 12 hours of cannabis smoking, supporting the use of oral THC tests as sensitive means to identify recent cannabis intake.

Results

EPOCH assay design

Figure 1 summarizes the EPOCH assay. The EPOCH test module (Figs. 1A, B) comprises an oral fluid processing kit, a sensor cartridge, and an optical detection cradle. For cost-effective mass production, we designed disposable parts, the processing unit and the cartridge, to be compatible with plastic injection-molding production (see Methods for details), and optimized their layouts to meet the machine tooling factors. We also developed a smartphone app to provide a one-touch user interface for image acquisition, automated image analysis, and data storage in a cloud server (Methods; Fig. S1).

The EPOCH test starts with oral fluid sampling using an oral swab. The swab is then inserted into the processing kit for oral fluid extraction and mixing with gold nanoparticles coated with THC antibodies ($AuNP_{Ab}$). The mixture is then dispensed onto the detection cartridge housing membrane sensors, and the optical signal from captured $AuNP_{Ab}$ is read out. EPOCH's membrane sensor employs a competitive immunoassay scheme (Fig. 1C), which is ideally suited to detecting small molecules. After the EPOCH assay is initiated, $AuNP_{Ab}$ first capture THC molecules in oral fluid. The THC-$AuNP_{Ab}$ complexes then pass through the membrane wherein THC competitors are spotted. We used THC haptens attached to bovine serum albumin (BSA) carriers as the competitor (THC_{BSA}). With high THC concentrations in oral fluid, most THC-binding sites on $AuNP_{Ab}$ would be occupied. This would lead to very few $AuNP_{Ab}$ being captured by THC_{BSA}, resulting in high light transmission. The entire assay, from sample to answer, completes within 5 minutes and requires <100 μL of oral fluid from a single swab.

Oral fluid processing

The processing kit performs multiple pre-analytical steps with a simple manual actuation (Fig. 2A and Fig. S2). The first step actuates a plunger (P1) in an extraction cylinder (Fig.

2B, **left**). In a single twist motion, oral fluid is drawn out from a swab, passes through an inline filter (0.45 μm pore), and collects in a metering reservoir with a fixed retention volume (20 μL). At the end of the P1 actuation, the reservoir rotates 90° to make a fluidic connection to a pumping chamber (Fig. 2B, **right**). The second twist motion (P2) through the air chamber then combines the collected oral fluid with preloaded $AuNP_{Ab}$ (50 μL) and pushes them via a mixing channel. Finally, the mixture is dispensed as two aliquots (~35 μL each), one for control check and the other for THC detection; the sensor cartridge aligns with the oral fluid processing kit's outlets for seamless sample transfer. The modular oral fluid kit not only expedites sample processing (1 min) but also facilitates reliable sample preparation for robust measurements. The inline filtration clears debris from oral fluid (Fig. 2C) to improve the sample's flow-through in the membrane sensors, and the metering mechanism ensures consistent stoichiometry, rendering the assay quantitative and inter-comparable.

Membrane sensor construction

We optimized the membrane sensor both for assay speed and sensitivity. The sensor consists of a membrane pad sandwiched between plastic sealing films for structural support (Fig. 3A and Fig. S3). $AuNP_{Ab}$-oral fluid mixture is injected through a small inlet (diameter, d_i) located at the membrane center; this structure confines the input sample to the small sensing zone (Fig. 1C), intensifying the analytical signal. We mounted two membrane sensors in a single cartridge: a test sensor to detect THC in oral fluid and a control sensor to validate sample loading.

Assay kinetics inside the membrane was our first area of improvement. Securely immobilizing binding competitor (THC_{BSA}) at the membrane center was shown to enhance overall $AuNP_{Ab}$ binding efficiency, thereby producing high optical signal. The conventional approach of directly spotting THC_{BSA} on a membrane, however, resulted in diffusive smaller signal spots, likely due to the loss of THC_{BSA} during immobilization. Increasing the effective molecular weight of THC_{BSA} was found to be effective: we mixed anti-immunoglobulin G antibodies (IgG_{Ab}) with anti-BSA antibodies (BSA_{Ab}) and then added THC_{BSA} (Fig. 3A **inset** and Table S2). This configuration produced the highest signal (Fig. S4). As for a membrane type, we tested membranes of different materials, such as nitrocellulose, polytetrafluoroethylene, polyvinylidene fluoride, and mixed cellulose ester, evaluating their assay compatibility and product reliability. We chose to use mixed cellulose ester (MCE) over the more commonly used nitrocellulose: MCE membranes produced more consistent and higher signals (Fig. S5) and were available from multiple commercial vendors.

Design optimization

To further guide our sensor design, we modeled the fluidic behavior in porous membranes (see Supporting Note for details; Fig. S6). By comparing different geometries, we found that a disk shape supports higher fluidic flow than conventional narrow strips (Fig. S7); the wetting front, where the capillary force drives fluids, radially expands in the disk shape but remains the same in a strip design. For a given disk, the overall flow rate (Q_R) increased with inlet size (d_i). In addition, Q_R was linearly proportional to membrane pore size (see

Supporting Note for details), which matched experimental observations (Fig. 3B). These results allowed us to define the minimal pore size required to meet the given assay speed. For example, to achieve the assay time of <3 minutes (or Q_R > 6 μL/min), the minimum pore size was 0.7 μm with d_i = 0.35 mm (shaded region in Fig. 3B).

In finalizing the sensor design, we carefully considered the balance between assay speed and reaction time; using a large-pore membrane supports higher flow (faster assay) but increases the risk of $AuNP_{Ab}$'s exit before binding to THC_{BSA} (lower sensitivity). Improving $AuNP_{Ab}$-binding rates thus favored using a small-pore membrane, which was equivalent to keeping low Péclet number (*Pe* = [diffusive transport time] / [advective transport time]). We estimated *Pe* for different radial sensor candidates (Fig. 3C) and imposed the relatively fast diffusion condition (*Pe* < 1, shaded region in Fig. 3C). Combining these criteria, namely, Q_R > 6 μL/min and *Pe* < 1, determined the optimal pore range (0.7 to 1 μm) for a given inlet diameter. Among commercially available membranes, we chose a 0.8-μm pore MCE membrane and set d_i = 0.35 mm for the lowest *Pe*. At a fixed assay time (3 min), the 0.8-μm membrane sensor indeed showed the highest signal intensity (Fig. 3D).

Detection optics

We next moved on to setting EPOCH's signal detection method. Light absorption by immobilized $AuNP_{Ab}$ (λ_{peak} = 525 nm) on a membrane could be detected through either the reflection or the transmission optics. We estimated the signal intensity from each mode by applying the Kubleka-Munk theory of light propagation in turbid media (see Supporting Note for details; Fig. S8) (28, 29). The model predicted that the transmission mode produces more substantial signal changes with varying AuNP concentrations (Fig. 3E), which is primarily due to the enhanced light transmittance through a wet membrane (30). Experimental data confirmed this prediction with the transmission mode achieving higher sensitivity and resolution (Fig. 3F). Based on these results, we designed the detection cradle that housed transmission optics and had a docking site for a smartphone (Fig. S9). The sensor cartridge was inserted to the cradle for optical alignment with a light-emitting diode (LED), a macro lens, and a smartphone camera. A sensing spot was then imaged by taking a close-up shot of transmission signals from the membrane sensor.

EPOCH assay characterization

We first determined the binding kinetics between $AuNP_{Ab}$ and its intended targets, THC and THC_{BSA}, via isothermal titration calorimetry (see Methods for details; Fig. S10). The measured association constant (K_a) between THC and $AuNP_{Ab}$ was 0.074 nM^{-1}. A similar value was observed (K_a = 0.073 nM^{-1}) between THC_{BSA} and $AuNP_{Ab}$. These results support the use of THC_{BSA} as an equivalent competitor to THC in the assay design. Under the EPOCH assay condition, temporal signal evolution with $AuNP_{Ab}$ binding on the membrane showed first-order Langmuir adsorption kinetics (Fig. 4A). The assay approached the equilibrium much more quickly than conventional enzyme-linked immunosorbent assay (ELISA) does; using the porous membrane effectively enhanced $AuNP_{Ab}$'s diffusive transport to their binding sites, so that the assay was limited mainly by the binding reaction alone. This reasoning was further supported by estimating the Damköhler (D_a) number, which measures the ratio between reaction and mass-transport rates (31). For the EPOCH

assay, D_a was ~0.06 (see Supporting Note for details), indicating that diffusive transport was not a limiting factor in $AuNP_{Ab}$ binding.

For a given sample, we measured two signals in the sensor cartridge, one from the THC test spot and the other from a control spot. The control signal validates that the $AuNP_{Ab}$-oral fluid mixture successfully loads on the membrane. We defined the EPOCH signal value (I_{EPOCH}) as the relative intensity change induced by membrane-bound $AuNP_{Ab}$ against the membrane background (see Methods for details; Fig. S11). Time-course I_{EPOCH} revealed that the assay's resolving power reached its maximum around 3 minutes after the assay began (Fig. 4B); accordingly, we set the detection window to 3 minutes after sample injection. Applying these protocols, we analyzed the THC-dilution series both in pure buffer and oral fluid (Fig. 4C). The EPOCH assay has detection limits of 0.12 ng/mL (buffer) and 0.17 ng/mL (oral fluid), both lower than the DRUID guideline of 1 ng/mL. The assay output was quantitative, with a dynamic range spanning about 4 orders of magnitude. EPOCH's analytical results matched those of GC-MS, the gold standard (Fig. 4D). The EPOCH assay, however, was faster (5 min vs. several hours), required no complex equipment, and performed without extensive sample preparations (see Methods for GC-MS sample preparation).

We further investigated how potential confounding variables such as drinking coffee, smoking cigarettes, consuming beer, and rinsing with mouth-wash affect the EPOCH signal. To compare samples, we asked non-cannabis users to complete these activities and immediately provide oral fluid samples, and spiked them with two different THC doses (1 and 10 ng/mL). The EPOCH tests were found to be robust in these different oral fluid conditions (Fig. 4E). At a given THC concentration, we observed statistically identical signal intensities among different oral fluid types (Fig. S12). Furthermore, the measured signal was significantly higher ($P = 0.0005$, one-sided t-test) than background even at low THC dose (1 ng/mL).

Detecting THC in cannabis users

Finally, we applied the EPOCH assay for on-site THC detection. We collected and tested oral fluid samples from recreational cannabis users (40 cannabis smokers and three THC-jelly users) within 10 minutes of product consumption. As a control, we also assessed oral fluid samples from non-cannabis users (13 traditional tobacco smokers and 30 non-smokers) without a history of cannabis use. In all cannabis-user samples, the EPOCH tests detected oral THC in concentrations that far exceeded the recommended guideline of 1 ng/mL (Fig. 5A); the average oral THC concentration was found to be 478 ng/mL for cannabis smokers and 138 μg/mL for jelly consumers. Oral THC concentrations of cannabis users were significantly higher than those of conventional tobacco smokers and non-smokers (all $P < 0.001$, Dunn's multiple comparison test), whereas THC concentrations of the latter two control groups were not significantly different ($P > 0.99$, Dunn's multiple comparison test; Fig. 5B). We observed no significant difference between male and female subjects in any of the cohorts ($P > 0.05$, two-sided Mann-Whitney test; Fig. 5C and Fig. S13).

We also monitored how THC concentrations changed over time after cannabis smoking. In this case, oral fluid samples were collected hourly after the inhalation and subjected to

the EPOCH tests. We observed that oral THC concentrations rapidly decreased (Fig. 5D), although the values were still >1 ng/mL six hours after the smoking. The estimated half-life of THC in oral fluid was 1.4 hours (Fig. 5E), in agreement with GC-MS measurements (32, 33). Combined with the initial THC average concentration (478 ng/mL), the decay kinetics indicated that oral THC concentrations likely stay above 1 ng/mL in the first 12 hours after cannabis smoking.

Discussion

Cannabis is currently approved for medicinal purposes in 36 US states and for recreational use in 15 (34). Given the legalization of THC consumption and the growing number of shops selling a variety of merchandise, the number of cannabis users is on the rise. Easy accessibility to THC containing products raises concerns regarding misuse (for example, overuse/overindulgence and consumption by minors) and accidents under its influence. The increasing potency of cannabis-related matters also poses threats to public safety (35). Consequently, it would be desirable to have rapid quantitative tests to measure and monitor THC concentrations in individuals. We developed the EPOCH system to help mitigate such THC-associated risks. EPOCH has the following advantages: i) the assay is fast (3-min sample-in-result-out) and robust to common interfering factors found in oral fluid; ii) it produces quantitative data comparable to GC-MS; iii) the detection limit (0.17 ng/mL) is below the regulatory guideline (1 ng/mL); and iv) the injection-molded cartridge and compact detection system enable on-site testing. In a proof-of-concept study using oral fluid samples from cannabis smokers and non-smokers, the EPOCH tests achieved excellent accuracy.

Several engineering features resulted in the notable analytical capabilities of EPOCH. First, we explored an advanced cartridge design, a disk-shaped MCE membrane with a small orifice inlet. This geometry supported a higher flow rate (thereby faster assay) than a conventional strip design, while at the same time concentrating input samples to a small sensing area (high signal density). Based on an analytical model for the fluidic behavior, we also optimized design parameters such as disk radius, inlet size, and membrane types, to achieve fast assay speed (<3 min) and high sensitivity (<1 ng/mL). Second, the pre-processing kit not only simplified sample handling but also kept the optimal stoichiometry between oral fluid (20 μL) and reagents ($AuNP_{Ab}$, 50 μL). This capacity promoted assay reproducibility and enabled THC quantification and comparison among different samples. Third, we adopted transmission optics for signal detection, exploiting the enhanced light penetration in a wet membrane. Both theoretical calculations and experimental data confirmed that the transmission mode generated larger signal changes than conventional reflective detection. Together, these technical advances effectively transformed qualitative lateral flow assays into fast, quantitative analytical tests, while using off-the-shelf raw materials that are readily available.

The EPOCH approach has technical advantages over electrochemical sensing, an alternative method for on-site THC testing (36) (see Table S3 for comparison). Since THC is a small molecule, it is difficult to adapt conventional immunoassays that use a pair of antibodies for THC capture and signal generation, respectively. Therefore, electrochemical sensors usually

are based on intrinsic THC redox reaction (37, 38), indirect chemical reactions (39, 40), or impedance spectroscopy (41) for signal generation; these methods tend to be sensitive to media conditions, including electrolyte composition, presence of metabolites, and pH, which can interfere with electrical measurements. The optics-based EPOCH is robust to such interfering factors and maintains high specificity of an immunoassay. The binding kinetics are also faster in EPOCH, as it confines target analyte in nanoscale pores and thereby shortens the time for target capture (see Supporting Note for details; Fig. 3C).

Oral fluid is an appealing alternative to urine as a drug-testing matrix. From the logistics aspect, oral fluid can be collected at almost any location and under observation, minimizing the chance of alteration. More importantly, THC concentrations in oral fluid reflect those in blood after cannabis smoking or vaping (42, 43) but are not influenced by oral intake of therapeutic capsules, for example dronabinol (44). Measuring THC in oral fluid is also less prone to concentration-dependent effects occurring in urine. As such, high oral THC concentrations can be a valid indicator of recent cannabis use and potential drug-induced impairment (45, 46). Combined with EPOCH's speed and simplicity, the oral THC test has the potential to become a practical surveillance tool. We do, however, recognize the need for further studies to obtain robust performance statistics. These include i) analyzing samples from second-hand THC smokers (47, 48); ii) testing the effect of other THC analogs, for example Δ^8-THC, on EPOCH results (49, 50); and iii) monitoring more time-lapse samples to refine drug's half-life in saliva (32, 33). Moreover, although not tested here, the EPOCH analysis could also be applied to other bodily fluids. For example, testing breast milk, wherein lipophilic THC can accumulate at high concentrations (51), could prevent babies' inadvertent exposure to THC. EPOCH could also be used to evaluate the THC content of cannabis products to safeguard users against accidentally consuming highly concentrated THC products.

The current study has the following limitations, and we envision a few future developments. First, separate modules in the current prototype need to be integrated into a single automated device, which will enhance assay throughput and reliability. We could also consider augmenting EPOCH by incorporating on-screen cognitive function tests, such as the digit symbol substitution test (DSST), which can be administered while the oral fluid assay is in progress (52, 53). As in the case of alcohol testing, combining molecular and cognitive tests would enable a more accurate assessment of drug-induced impairment. Second, we need to expand our longitudinal study of cannabis smoking with more frequent sampling and larger cohorts, which will produce robust statistical data on THC pharmacodynamics in oral fluid. Third, the cybersecurity feature of the current app will have to be upgraded to meet legal requirements, such as Health Insurance Portability and Accountability Act (HIPAA). This can be achieved by adopting a managed database service for data transfer and app distribution. Fourth, we may adopt signal-amplification approaches to further boost assay sensitivity. For qualitative tests, we could deposit metallic silver over AuNPs; this process will lower the detection limit (about 10-fold) by intensifying optical density at the detection spots (54). Using other types of engineered-nanomaterials, such as Au nanocages (55) and multimeric Au complexes (56), would be an alternative way to intensify optical signal while maintaining analytical resolution. These strategies would render the EPOCH assay comparable to ELISA in sensitivity but much faster in assay turnaround (<5 min vs.

1–3 hours). Finally, testing targets could be expanded to include a broader panel of drugs. Besides THC, other psychoactive substances, including opiates, amphetamines, cocaine, and benzodiazepines, have been shown to be present in oral fluid after their recent use (21). It is thus conceivable to run on-site, multi-panel EPOCH tests from a single oral fluid specimen to rapidly identify drug types and initiate treatment for overdoses, for example naloxone for opiates. These developments will position EPOCH as a cost-effective, versatile analytical platform with applications in roadside and emergency situations as well as workplaces, sports, and laboratories.

Materials and methods

Study design

The goal of this study was to develop a rapid, quantitative method for detecting THC concentrations in oral fluid, with the aim of providing on-site tests for cannabis smoking. We hypothesized that adopting a filter membrane with a radial flow would improve the assay speed and sensitivity compared to the conventional lateral flow design (a rectangular strip). We collected oral fluid samples from adults (over the age of 21) cannabis smokers in Massachusetts, US. Cannabis smokers were asked to collect oral fluid after their usual cannabis consumption to get high or stoned. Each smoker used his or her own cannabis supply, and the intake method was restricted to smoking only. For the screening experiment, the oral fluid collection window was within 10 minutes after cannabis smoking. In case of the serial monitoring, three participants hourly collected oral fluid after their initial cannabis smoking. No additional consumption of cannabis nor food was requested. For edible product users, we asked them to collect oral fluid within 10 minutes after consuming one or two THC-containing jellies (THC concentration >5 mg/piece). The control groups were healthy volunteers with no history of drug use or recent medication. Study participants, who met eligibility criteria and gave informed consent, were recruited on a rolling basis (randomization non-applicable). The samples were from cannabis users ($n = 43$) and controls ($n = 43$), to obtain confidence interval (CI) for sensitivity (from cannabis users) and specificity (from controls). The sample size of ≥40 per each cohort was calculated to set 95% CI ≤ 0.1. With 43 cannabis-user samples, the observed sensitivity was 100% and the estimated CI 92–100%; with 43 controls, the observed specificity was 100% and the estimated CI 92–100% (Clopper-Pearson method). All samples were measured at least 3 times (technical replica), and the mean values were used for analyses. The sample source and test results were blinded until the statistics analyses. No data were excluded. This study was approved by the Institutional Review Board of Massachusetts General Hospital (IRB number 2019P003472, PI: Hakho Lee), and the overall procedures followed institutional guidelines.

Sample collection

Self-administering cannabis users with their own supply were asked to collect oral fluid samples within 10 minutes after smoking or THC-jelly consumption. Specifically, the users were instructed to take a disposable swab (diameter, 1 cm; length, 1.5 cm) into the mouth and roll it around for about one minute. Control samples were collected in the same manner from volunteers who self-declared no history of recent or prior cannabis consumption. For

the time-course monitoring, three cannabis smokers collected oral fluid samples hourly after their last smoking. We purchased cylindrical oral swabs (SalivaBio Oral Swab, Salimetrics). These swabs were cut in the middle of their length to fit into the sample processing kit. Each halved swab collected about 0.5 mL of oral fluid.

Preparing gold nanoparticles conjugated with THC antibodies

We tested three THC antibodies (10–1388, Fitzgerald; 10-T43G, Fitzgerald; MBS568010, MyBioSource) and chose the one (10–1388) that showed the highest sensitivity in the EPOCH assay. 10 μL of 1 mg/mL THC antibody was added to a mixture of 1 mL of gold nanoparticles (diameter, 20 nm; BBI solutions) and 100 μL of 0.1 M borate buffer (ThermoFisher Scientific). After incubation at 20 °C for an hour, 10 μL of 10% protein saver (Toyobo) was added to the mixture to block the unreacted gold nanoparticle surface. The mixture was again incubated at 20 °C for an hour and then centrifuged (8000 × g) at 10 °C for 15 minutes. The supernatant was discarded, and the pellets were re-suspended in 10 mM borate buffer. The centrifugation and re-suspension were repeated two more times. The final $AuNP_{Ab}$ solution was prepared with 1% polyvinylpyrrolidone (MilliporeSigma), 0.5 % surfactant 10G (Fitzgerald), and 1% dimethyl sulfoxide (MilliporeSigma) in phosphate-buffered saline (PBS) buffer. About seven THC antibodies were adsorbed on a single particle, and the conjugated particles were stable for at least 2 weeks at ambient storage conditions (Fig. S14).

Sample processing kit

The device was designed to be injection-molded for mass production. For fast prototyping, we fabricated mockup devices via mechanical machining. Polycarbonate, which is one of the plastic materials for injection-molding, was used as a structural material and machined via micro-milling (100 μm micro-end mill). The sample processing kit is divided into four parts: two inner halves for sample processing and two outer halves for sample storage. The assembled kit (24 × 60 × 65 mm^3) has two chambers, one for the oral swab and the other for pumping. Each chamber is fitted with a plunger that can be manually actuated through twisting motions. Other key design features are: (i) the swab chamber includes an inline filter (pore size, 0.45 μm; HAWP02500, MilliporeSigma) to remove debris from natural oral fluid; (ii) the oral fluid reservoir has overflow openings to collect a fixed volume of oral fluid (20 μL). The collected oral fluid then mixes with $AuNP_{Ab}$ (50 μL) that were preloaded into the device. $AuNP_{Ab}$ are retained under the oral fluid reservoir with off-axis flow alignment with the reservoir outlet (see Fig. S2 for details); (iii) the fluidic channel has a beehive-like expansion structure to enhance the mixing efficiency between oral fluid and $AuNP_{Ab}$ (57–59); and (iv) the two processing kit outlets line up with the sensor cartridge inlets for seamless sample delivery.

EPOCH sensor cartridge

The cartridge has two parts, a bottom tray and a cover plate, that were produced via injection molding. These parts interlock mechanically by snap-fit (Fig. 3A) for easy assembly and uniform contact between membrane sensors and plastic parts. Each cartridge contains two membrane sensors, one as control and the other to test THC. The control assay membrane is spotted with 1 μL of anti-mouse IgG antibody (M8642, MilliporeSigma) to capture

AuNPs conjugated with THC antibodies. The test membrane is spotted with a mixture of anti-mouse IgG antibody (M8642, MilliporeSigma), anti-BSA antibody (ab3781, Abcam, UK), and THC_{BSA} (80–1051, Fitzgerald). The ratio between antibodies and hapten was experimentally optimized (see Table S2). Each sensor is made of a 0.8-μm MCE membrane (diameter, 20 mm; AAWP02500, MilliporeSigma) sandwiched between two plastic films (SealPlate® film, MilliporeSigma). A 0.35-mm inlet hole was punched at the center of the top film before the lamination. A pair of sensors (control and THC test) was placed on an additional film (41 × 20 mm^2; SealPlate®) to fix their relative spacing. The assembly was installed in the cartridge, keeping the sensor inlets aligned with the cartridge openings. The cartridge was then put in a convection oven at 37 ℃ for an hour for drying.

Optical detection device

The cradle (80 × 85 × 65 mm^3) houses a printed circuit board for a 525-nm LED (XPEBGR, Cree Inc.), a convex lens (LB1844-A, Thorlabs), a push-button switch for an LED on-off control, and a 9 V battery (Fig. S9). The cradle was also designed to function as a base stand for signal measurements; it docks with a smartphone (Galaxy S5, Samsung), has an insert for the sensor cartridge, and provides a lightproof dark environment. When the system is fully installed, the rear-facing phone camera, the lens, the THC detection spot in the sensor cartridge, and the LED are aligned to get the transmission sensing image. Using the lens (focal length, 5 cm) allows the camera to take a close-up of the detection spot simultaneously, shortening the working distance between the camera and the sensor cartridge (3.5 cm). The phone is inserted into the cradle upside-down, which decreases the overall cradle size.

Smartphone app

We developed a smartphone app for image acquisition and data analyses (Fig. S1). For image analyses, the program automatically defines five regions of interest (ROIs) in a grayscale image: one ROI_{AuNP} for the detection spot where $AuNP_{Ab}$ are bound and the other four ROI_{REF} as a background reference (Fig. S11). The area of the ROI_{AuNP} is the same as the area sum of the four ROI_{REF}. For each ROI, the total pixel intensity is obtained, I_{AuNP} from ROI_{AuNP}, and I_{REF} from four ROI_{REF}. As an analytical metric, the EPOCH signal value (I_{EPOCH}) is calculated as $I_{EPOCH} = (I_{REF} - I_{AuNP})/I_{REF}$. The app has an internal lookup table to convert I_{EPOCH} to an estimated THC concentration in oral fluid. For each test, the app stored raw images, ROI information, and geolocation data in a cloud server using the phone's wireless connection. For encrypted communications between clients and servers, we used the transport layer security (TLS) functions. The app was written in a programming language, Java, using Android Studio.

Binding kinetics

We used isothermal titration calorimetry (ITC) to measure binding interactions in the following pairs: i) THC and $AuNP_{Ab}$; ii) THC_{BSA} and $AuNP_{Ab}$; and iii) THC_{BSA} and $AuNP_{Ab}$ complexed with THC. Prior to ITC, buffers of THC, THC_{BSA} and $AuNP_{Ab}$ were changed into 5% dimethyl sulfoxide (DMSO) in 1× PBS. THC (1 mg/mL) in methanol was heated to 45 °C (2 hours) to evaporate methanol, and DMSO was added to make 4 mM THC solution. The solution was diluted in 1× PBS to obtain 200 μM [THC] in 5%

DMSO. THC_{BSA} (17.03 mg/mL) was buffer-exchanged and made to 300 μM THC_{BSA} in 5% DMSO. $AuNP_{Ab}$ solution was prepared as described above, and the buffer was changed to 5% DMSO in 1× PBS. For ITC measurements, we used MicroCal PEAQ-ITC (Malvern). The injection syringe was filled with either THC or THC_{BSA}; the sample cell was filed with $AuNP_{Ab}$ solution or $AuNP_{Ab}$ pre-complexed with THC. Titrant was injected from the syringe to the sample cell, with one initial injection of 0.4 μL followed by 11 injections of 2 μL (THC to $AuNP_{Ab}$, THC_{BSA} to THC-$AuNP_{Ab}$ complex) or 1.5 μL (THC_{BSA} to $AuNP_{Ab}$). The sample cell was continuously stirred at 750 rpm. The obtained data were analyzed by MicroCal PEAQ-ITC Analysis Software (Malvern).

Gas chromatography–mass spectrometry

Due to a regulatory restriction, we used tetrahydrocannabivarin (THCV; T-094, Cerilliant), an analog of THC, as a standard material for GC-MS (7890B-5977A, Agilent Technologies, US). The initial THCV (1.0 mg/mL) was two-fold serially diluted with methanol (MilliporeSigma) to 1.0 ng/mL. The dilute THCV samples were injected into GC-MS using an auto-sampler system (PAL, Agilent Technologies) with a 10 μL syringe at an injection volume of 2 μL. About 80% of the syringe volume was filled with methanol for the pre-cleaning process before measurement, followed by sample injection at a speed of 50 μL/s. The pre- and post-injection delays were each 500 ms. Initial GC temperature was set to 30 °C, and the temperature gradually rose at a rate of 30 °C/min until it reached 325 °C. GC column (19091S-433, Agilent Technologies) was utilized with 6.4845 psi pressure, 1 mL/min phase moving speed (average speed of 36.074 cm/sec), resulting in 1.386 min holding time. The acquisition mode was set to SIM/scan method. For comparison, we also designed the membrane sensor for THCV and obtained a dose-dependent titration curve (Fig. S15).

Statistics.

Statistical analysis was performed using GraphPad Prism version 9.0 (GraphPad Software Inc.) or R version 3.6.1. For all statistical tests, P values < 0.05 were considered significant. We used Student t-test to compare two groups. Multiple (≥3) groups were compared via analysis of variance (ANOVA), followed by Dunn's multiple comparison test.

Supplementary Material

Refer to Web version on PubMed Central for supplementary material.

Acknowledgments:

The authors thank Keywhan Chung (University of Illinois at Urbana-Champaign, IL, US) and Naebong Jeong (Massachusetts General Hospital, MA, US) for helpful discussion; Dr. Michelle Garlin (Massachusetts General Hospital) and Sae-Young Cheon (University of Southern California, CA, US) for helpful discussion on graphic designs and illustrations; and Dr. Kaley Joyce for critically reading the manuscript.

Funding:

We acknowledge the following grant support: NIH R21DA049577 to Hakho L., R01CA229777 to Hakho L., R01CA204019 to R.W., U01CA233360 to Hakho L. and C.M.C., R01CA239078 to Hakho L., R01CA237500 to Hakho L., R01CA264363 to C.M.C., DOD-W81XWH1910199 to Hakho L., DOD-W81XWH1910194 to Hakho L, Robert Wood Johnson Foundation to C.M.C., American Cancer Society to C.M.C., MGH Scholar Fund to Hakho

L., National Research Foundation (South Korea) 2017R1A2B3010816 to M.-G.K., and the Institute for Basic Science Grant (South Korea) IBS-R026-D1 to Jinwoo C.

Data and materials availability:

All data needed to evaluate the conclusions in the paper are present in the paper and/or the Supplementary Materials. Materials are available upon request by contacting the corresponding author.

References and Notes

1. Key substance use and mental health indicators in the United States: results from the 2018 national survey on drug use and health (Substance Abuse and Mental Health Services Administration, MD, USA, 2019).
2. Katz-Talmor D, Katz I, Porat-Katz BS, Shoenfeld Y, Cannabinoids for the treatment of rheumatic diseases - where do we stand. Nat. Rev. Rheumatol 14, 488–498 (2018). [PubMed: 29884803]
3. Hill KP, Palastro MD, George TP, Therapeutic cannabis use in 2018: where do we stand. Lancet Psychiatry 6, 88–89 (2019). [PubMed: 30686389]
4. Hall W, Degenhardt L, Adverse health effects of non-medical cannabis use. Lancet 374, 1383–1391 (2009). [PubMed: 19837255]
5. Meier MH, Docherty M, Leischow SJ, Grimm KJ, Pardini D, Cannabis concentrate use in adolescents. Pediatrics 144, e20190338 (2019). [PubMed: 31451609]
6. Murray RM, Morrison PD, Henquet C, Di Forti M, Cannabis, the mind and society: the hash realities. Nat. Rev. Neurosci 8, 885–895 (2007). [PubMed: 17925811]
7. Moore THM, Zammit S, Lingford-Hughes A, Barnes TRE, Jones PB, Burke M, Lewis G, Cannabis use and risk of psychotic or affective mental health outcomes: a systematic review. Lancet 370, 319–328 (2007). [PubMed: 17662880]
8. Hartman RL, Huestis MA, Cannabis effects on driving skills. Clin. Chem 59, 478–492 (2013). [PubMed: 23220273]
9. Fergusson DM, Horwood LJ, Boden JM, Is driving under the influence of cannabis becoming a greater risk to driver safety than drink driving? Findings from a longitudinal study. Accid. Anal. Prev 40, 1345–1350 (2008). [PubMed: 18606265]
10. Veldstra JL, Bosker WM, De Waard D, Ramaekers JG, Brookhuis KA, Comparing treatment effects of oral THC on simulated and on-the-road driving performance: testing the validity of driving simulator drug research. Psychopharmacology 232, 2911–2919 (2015). [PubMed: 25957748]
11. Hasin DS, Sarvet AL, Cerdá M, Keyes KM, Stohl M, Galea S, Wall MM, US adult illicit cannabis use, cannabis use disorder, and medical marijuana laws: 1991–1992 to 2012–2013. JAMA Psychiatry 74, 579–588 (2017). [PubMed: 28445557]
12. Hartley S, Simon N, Larabi A, Vaugier I, Barbot F, Quera-Salva M-A, Alvarez JC, Effect of smoked cannabis on vigilance and accident risk using simulated driving in occasional and chronic users and the pharmacokinetic–pharmacodynamic relationship. Clin. Chem 65, 684–693 (2019). [PubMed: 30872375]
13. Dahlgren MK, Sagar KA, Smith RT, Lambros AM, Kuppe MK, Gruber SA, Recreational cannabis use impairs driving performance in the absence of acute intoxication. Drug Alcohol Depend 208, 107771 (2020). [PubMed: 31952821]
14. Röhrich J, Schimmel I, Zörntlein S, Becker J, Drobnik S, Kaufmann T, Kuntz V, Urban R, Concentrations of Δ9-tetrahydrocannabinol and 11-nor-9-carboxytetrahydrocannabinol in blood and urine after passive exposure to cannabis smoke in a coffee shop. J. Anal. Toxicol 34, 196–203 (2010). [PubMed: 20465865]
15. Breidi SE, Barker J, Petróczi A, Naughton DP, Enzymatic digestion and selective quantification of underivatised delta-9-tetrahydrocannabinol and cocaine in human hair using gas chromatography-mass spectrometry. J. Anal. Methods Chem 2012, 907893 (2012). [PubMed: 22567573]

16. Verstraete AG, Detection times of drugs of abuse in blood, urine, and oral fluid. Ther. Drug Monit 26, 200–205 (2004). [PubMed: 15228165]
17. Andås HT, Krabseth HM, Enger A, Marcussen BN, Haneborg AM, Christophersen AS, Vindenes V, Øiestad EL, Detection time for THC in oral fluid after frequent cannabis smoking. Ther. Drug Monit 36, 808–814 (2014). [PubMed: 24819969]
18. Lee D, Milman G, Barnes AJ, Goodwin RS, Hirvonen J, Huestis MA, Oral fluid cannabinoids in chronic, daily cannabis smokers during sustained, monitored abstinence. Clin. Chem 57, 1127–1136 (2011). [PubMed: 21677094]
19. Desrosiers NA, Himes SK, Scheidweiler KB, Concheiro-Guisan M, Gorelick DA, Huestis MA, Phase I and II cannabinoid disposition in blood and plasma of occasional and frequent smokers following controlled smoked cannabis. Clin. Chem 60, 631–643 (2014). [PubMed: 24563491]
20. Anizan S, Milman G, Desrosiers N, Barnes AJ, Gorelick DA, Huestis MA, Oral fluid cannabinoid concentrations following controlled smoked cannabis in chronic frequent and occasional smokers. Anal. Bioanal. Chem 405, 8451–8461 (2013). [PubMed: 23954944]
21. Desrosiers NA, Huestis MA, Oral fluid drug testing: analytical approaches, issues and interpretation of results. J. Anal. Toxicol 43, 415–443 (2019). [PubMed: 31263897]
22. Milman G, Schwope DM, Gorelick DA, Huestis MA, Cannabinoids and metabolites in expectorated oral fluid following controlled smoked cannabis. Clin. Chim. Acta 413, 765–770 (2012). [PubMed: 22285315]
23. Odell MS, Frei MY, Gerostamoulos D, Chu M, Lubman DI, Residual cannabis levels in blood, urine and oral fluid following heavy cannabis use. Forensic Sci. Int 249, 173–180 (2015). [PubMed: 25698515]
24. Bosker WM, Huestis MA, Oral fluid testing for drugs of abuse. Clin. Chem 55, 1910–1931 (2009). [PubMed: 19745062]
25. Cirimele V, Villain M, Mura P, Bernard M, Kintz P, Oral fluid testing for cannabis: on-site Oraline® IV sat device versus GC/MS. Forensic Sci. Int 161, 180–184 (2006). [PubMed: 16854544]
26. Lee J-R, Choi J, Shultz TO, Wang SX, Small molecule detection in saliva facilitates portable tests of marijuana abuse. Anal. Chem 88, 7457–7461 (2016). [PubMed: 27434697]
27. Swortwood MJ, Newmeyer MN, Andersson M, Abulseoud OA, Scheidweiler KB, Huestis MA, Cannabinoid disposition in oral fluid after controlled smoked, vaporized, and oral cannabis administration. Drug Test. Anal 9, 905–915 (2017). [PubMed: 27647820]
28. Kubelka P, New contributions to the optics of intensely light-scattering materials. J. Opt. Soc. Am 38, 448–457 (1948). [PubMed: 18916891]
29. Wang JX, Nilsson AM, Fernandes DLA, Niklasson GA, Angle dependent light scattering by gold nanospheres. J. Phys.: Conf. Ser 682, 012018 (2016).
30. Swanson C, Lee S, Aranyosi AJ, Tien B, Chan C, Wong M, Lowe J, Jain S, Ghaffari R, Rapid light transmittance measurements in paper-based microfluidic devices. Sens. Biosensing Res 5, 55–61 (2015).
31. Squires TM, Messinger RJ, Manalis SR, Making it stick: convection, reaction and diffusion in surface-based biosensors. Nat. Biotechnol 26, 417–426 (2008). [PubMed: 18392027]
32. Kauert GF, Ramaekers JG, Schneider E, Moeller MR, Toennes SW, Pharmacokinetic properties of delta9-tetrahydrocannabinol in serum and oral fluid. J. Anal. Toxicol 31, 288–293 (2007). [PubMed: 17579974]
33. Toennes SW, Ramaekers JG, Theunissen EL, Moeller MR, Kauert GF, Pharmacokinetic properties of delta9-tetrahydrocannabinol in oral fluid of occasional and chronic users. J. Anal. Toxicol 34, 216–221 (2010). [PubMed: 20465868]
34. Das A, Johnson J, Hard G, Jones A, State Medical Marijuana Laws and Initiation of Cigarettes among Adolescents in the US, 1991–2015. Cannabis 4, 60–68 (2021).
35. World drug report 2019 (UNP Sales No. E.19.XI.8, United Nations Office on Drugs and Crime, Vienna, Austria, 2019).
36. Klimuntowski M, Alam MM, Singh G, Howlader MMR, Electrochemical Sensing of Cannabinoids in Biofluids: A Noninvasive Tool for Drug Detection. ACS Sens 5, 620–636 (2020). [PubMed: 32102542]

37. Renaud-Young M, Mayall RM, Salehi V, Goledzinowski M, Comeau FJE, MacCallum JL, Birss VI, Development of an ultra-sensitive electrochemical sensor for Δ9-tetrahydrocannabinol (THC) and its metabolites using carbon paper electrodes. Electrochim. Acta 307, 351–359 (2019).
38. Mishra RK, Sempionatto JR, Li Z, Brown C, Galdino NM, Shah R, Liu S, Hubble LJ, Bagot K, Tapert S, Wang J, Simultaneous detection of salivary Δ^9-tetrahydrocannabinol and alcohol using a Wearable Electrochemical Ring Sensor. Talanta 211, 120757 (2020). [PubMed: 32070607]
39. Wanklyn C, Burton D, Enston E, Bartlett CA, Taylor S, Raniczkowska A, Black M, Murphy L, Disposable screen printed sensor for the electrochemical detection of delta-9-tetrahydrocannabinol in undiluted saliva. Chem. Cent. J 10, 1 (2016). [PubMed: 26807144]
40. Goodwin A, Banks C, Compton R, Graphite Micropowder Modified with 4-Amino-2,6-diphenylphenol Supported on Basal Plane Pyrolytic Graphite Electrodes: Micro Sensing Platforms for the Indirect Electrochemical Detection of Δ9-Tetrahydrocannabinol in Saliva. Electroanalysis 18, 1063–1067 (2006).
41. Stevenson H, Bacon A, Joseph KM, Gwandaru WRW, Bhide A, Sankhala D, Dhamu VN, Prasad S, A Rapid Response Electrochemical Biosensor for Detecting Thc In Saliva. Sci. Rep 9, 12701 (2019). [PubMed: 31481686]
42. Milman G, Schwope DM, Schwilke EW, Darwin WD, Kelly DL, Goodwin RS, Gorelick DA, Huestis MA, Oral fluid and plasma cannabinoid ratios after around-the-clock controlled oral Δ9-tetrahydrocannabinol administration. Clin. Chem 57, 1597–1606 (2011). [PubMed: 21875944]
43. Pacifici R, Pichini S, Pellegrini M, Rotolo MC, Giorgetti R, Tagliabracci A, Busardò FP, Huestis MA, THC and CBD concentrations in blood, oral fluid and urine following a single and repeated administration of “light cannabis”. Clin. Chem. Lab. Med 58, 682–689 (2020). [PubMed: 30956228]
44. Childs E, Lutz JA, de Wit H, Dose-related effects of delta-9-THC on emotional responses to acute psychosocial stress. Drug Alcohol Depend 177, 136–144 (2017). [PubMed: 28599212]
45. Drummer OH, Drug testing in oral fluid. Clin. Biochem. Rev 27, 147–159 (2006). [PubMed: 17268583]
46. Lee D, Huestis MA, Current knowledge on cannabinoids in oral fluid. Drug Test. Anal 6, 88–111 (2014). [PubMed: 23983217]
47. Herrmann ES, Cone EJ, Mitchell JM, Bigelow GE, LoDico C, Flegel R, Vandrey R, Non-smoker exposure to secondhand cannabis smoke II: Effect of room ventilation on the physiological, subjective, and behavioral/cognitive effects. Drug Alcohol Depend 151, 194–202 (2015). [PubMed: 25957157]
48. Wei B, Smith DM, Travers MJ, O’Connor RJ, Goniewicz ML, Hyland AJ, Chapter One - Secondhand marijuana smoke (SHMS): Exposure occurrence, biological analysis and potential health effects. Adv. Mol. Toxicol 13, 1–30 (2019).
49. Gill AD, Hickey BL, Zhong W, Hooley RJ, Selective sensing of THC and related metabolites in biofluids by host:guest arrays. ChemComm 56, 4352–4355 (2020).
50. Casajuana Köguel C, López-Pelayo H, Balcells-Olivero MM, Colom J, Gual A, Psychoactive constituents of cannabis and their clinical implications: a systematic review. Adicciones 30, 140–151 (2018). [PubMed: 28492950]
51. Perez-Reyes M, Wall ME, Presence of delta9-tetrahydrocannabinol in human milk. N. Engl. J. Med 307, 819–820 (1982). [PubMed: 6287261]
52. Jaeger J, Digit symbol substitution test: the case for sensitivity over specificity in neuropsychological testing. J. Clin. Psychopharmacol 38, 513–519 (2018). [PubMed: 30124583]
53. Pham L, Harris T, Varosanec M, Morgan V, Kosa P, Bielekova B, Smartphone-based symbol-digit modalities test reliably captures brain damage in multiple sclerosis. NPJ Digit. Med 4, 1–13 (2021). [PubMed: 33398041]
54. Zhang Z, Li W, Zhao Q, Cheng M, Xu L, Fang X, Highly sensitive visual detection of copper (II) using water-soluble azide-functionalized gold nanoparticles and silver enhancement. Biosens. Bioelectron 59, 40–44 (2014). [PubMed: 24690560]
55. Yang Y, Ozsoz M, Liu G, Gold nanocage-based lateral flow immunoassay for immunoglobulin G. Microchim. Acta 184, 2023–2029 (2017).

56. Hu J, Wang L, Li F, Han YL, Lin M, Lu TJ, Xu F, Oligonucleotide-linked gold nanoparticle aggregates for enhanced sensitivity in lateral flow assays. Lab Chip 13, 4352–4357 (2013). [PubMed: 24056409]
57. Coleman JT, McKechnie J, Sinton D, High-efficiency electrokinetic micromixing through symmetric sequential injection and expansion. Lab Chip 6, 1033–1039 (2006). [PubMed: 16874374]
58. Shallan AI, Smejkal P, Corban M, Guijt RM, Breadmore MC, Cost-effective three-dimensional printing of visibly transparent microchips within minutes. Anal. Chem 86, 3124–3130 (2014). [PubMed: 24512498]
59. Plevniak K, Campbell M, Myers T, Hodges A, He M, 3D printed auto-mixing chip enables rapid smartphone diagnosis of anemia. Biomicrofluidics 10, 054113 (2016). [PubMed: 27733894]
60. Hong S, Kim W, Dynamics of water imbibition through paper channels with wax boundaries. Microfluid. Nanofluidics 19, 845–853 (2015).
61. Gong MM, Sinton D, Turning the page: advancing paper-based microfluidics for broad diagnostic application. Chem. Rev 117, 8447–8480 (2017). [PubMed: 28627178]
62. Jain PK, Lee KS, El-Sayed IH, El-Sayed MA, Calculated absorption and scattering properties of gold nanoparticles of different size, shape, and composition: applications in biological imaging and biomedicine. J. Phys. Chem. B 110, 7238–7248 (2006). [PubMed: 16599493]
63. Maheu B, Letoulouzan JN, Gouesbet G, Four-flux models to solve the scattering transfer equation in terms of Lorenz-Mie parameters. Appl. Opt 23, 3353 (1984). [PubMed: 18213168]
64. Wong K, Chen C, Wei K, Roy VAL, Chathoth SM, Diffusion of gold nanoparticles in toluene and water as seen by dynamic light scattering. J. Nanoparticle Res 17, 153 (2015).
65. Lowe ER, Banks CE, Compton RG, Indirect detection of substituted phenols and cannabis based on the electrochemical adaptation of the Gibbs reaction. Anal. Bioanal. Chem 383, 523–531 (2005). [PubMed: 16136302]
66. Balbino MA, Eleoterio IC, de Oliveira MF, McCord BR, Electrochemical study of delta-9-tetrahydrocannabinol by cyclic voltammetry using screen printed electrode, improvements in forensic analysis. Sens. Transducers 207, 73–78 (2016).
67. Zhang Q, Berg D, Mugo SM, Molecularly imprinted carbon based electrodes for tetrahydrocannabinol sensing. Inorg. Chem. Commun 107, 107459 (2019).

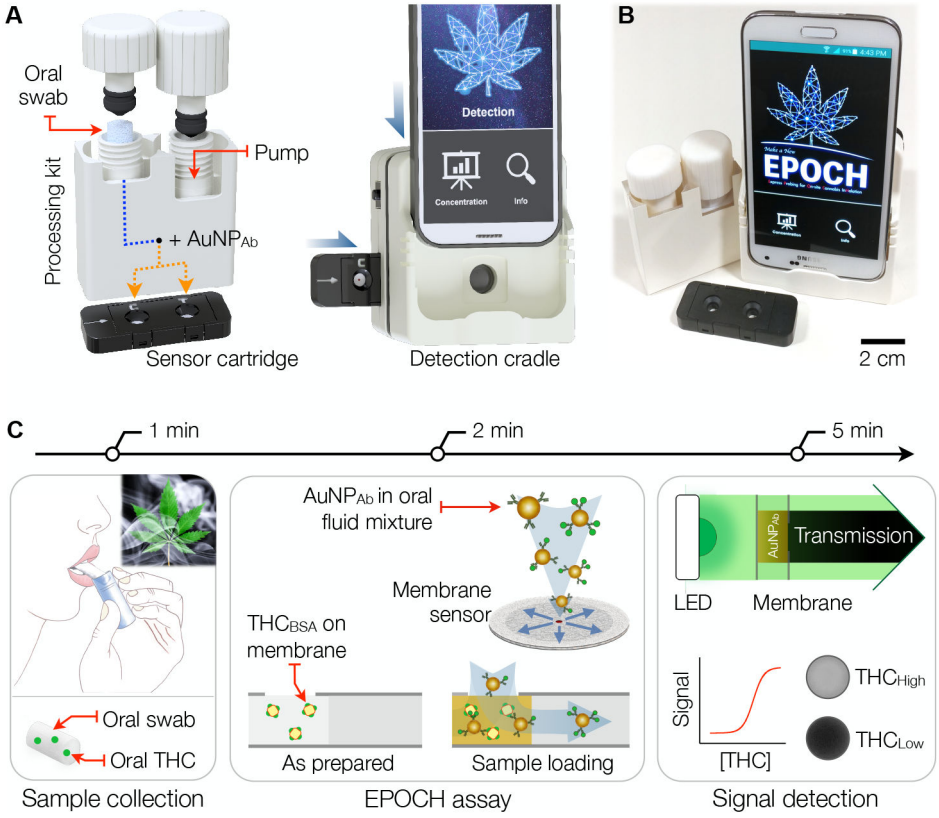

Fig. 1. EPOCH assay overview.

(A) The EPOCH system has three modules for on-site THC assay: i) a sample processing kit for extracting oral fluid and labeling with $AuNP_{Ab}$; ii) an injection-molded cartridge housing membrane sensors; and iii) a detection cradle for optical signal detection. The processing kit, paired with the sensor cartridge, delivers $AuNP_{Ab}$-oral fluid mixture to test and control sites. The sample-spotted cartridge is inserted into the cradle and imaged by a smartphone camera. **(B)** A photo of a compact prototype system. **(C)** 5-min THC detection. (Left) An oral-fluid sample is collected using a swab. (Middle) oral fluid is extracted and mixed with $AuNP_{Ab}$. The mixture is then spotted on a radial membrane sensor that has immobilized THC competitors (THC haptens conjugated to BSA carriers; THC_{BSA}). (Right) $AuNP_{Ab}$ differentially binds to THC_{BSA} according to oral THC concentration. Transmission through the sensing spot is digitized for THC quantification.

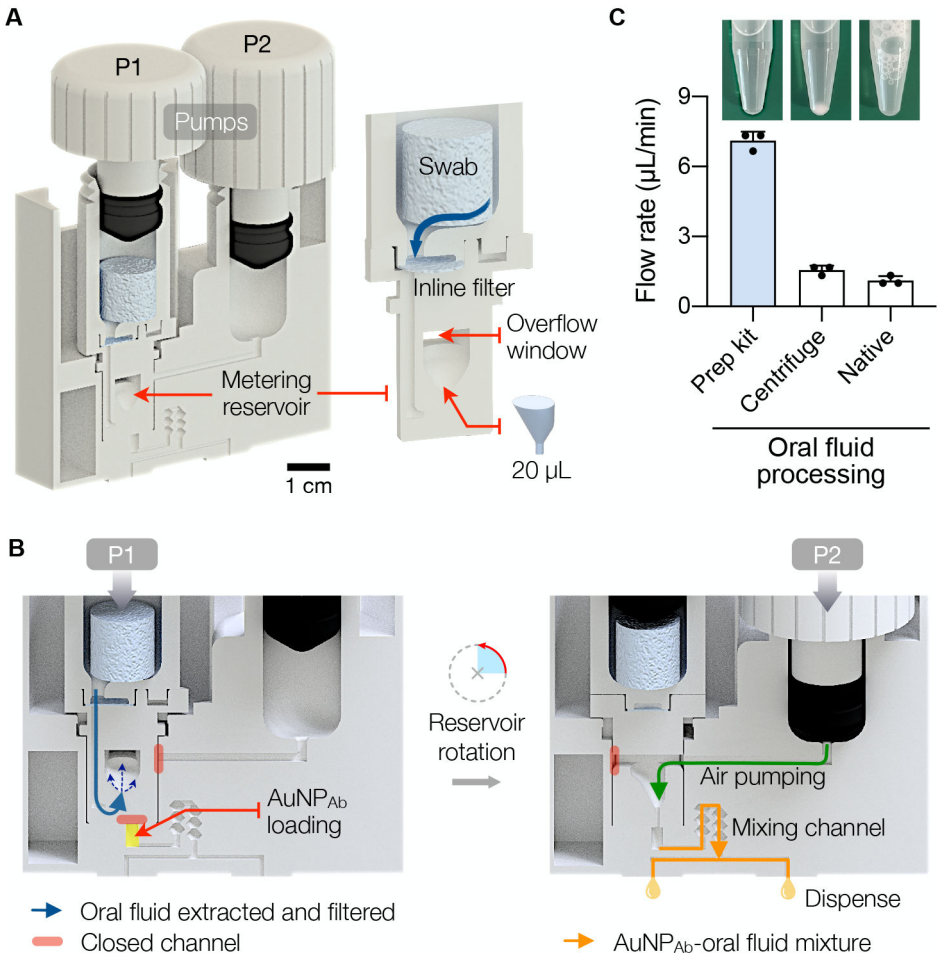

Fig. 2. EPOCH oral fluid processing.

(A) A sample processing kit designed to extract oral fluid and mix it with $AuNP_{Ab}$. The kit has two screw-type actuators (P1, P2) for pumping. The metering reservoir (right inset) removes oral debris thorough an inline filter (0.45 µm cut-off) and collects a fixed volume (20 µL) of oral fluid. **(B)** Two-step sample processing. Step 1, left: A user advances P1 through a twisting motion, which squeezes the oral swab and collects oral fluid in the reservoir. Excess fluid exits through the overflow window; paths to other fluidic channels are initially blocked. At the end of P1 twisting, the reservoir rotates 90° and makes a connection to the $AuNP_{Ab}$ chamber. Step 2, right: Twisting P2 transports oral fluid to $AuNP_{Ab}$ and pushes the mixture through the stirring channel. The final sample is divided and delivered to the detection cartridge. The operation time is 1 minute. **(C)** Oral fluid samples purified by the processing kit flowed through porous membranes faster than centrifuged or native oral fluid samples. The bar represents mean ± SD from technical triplicates.

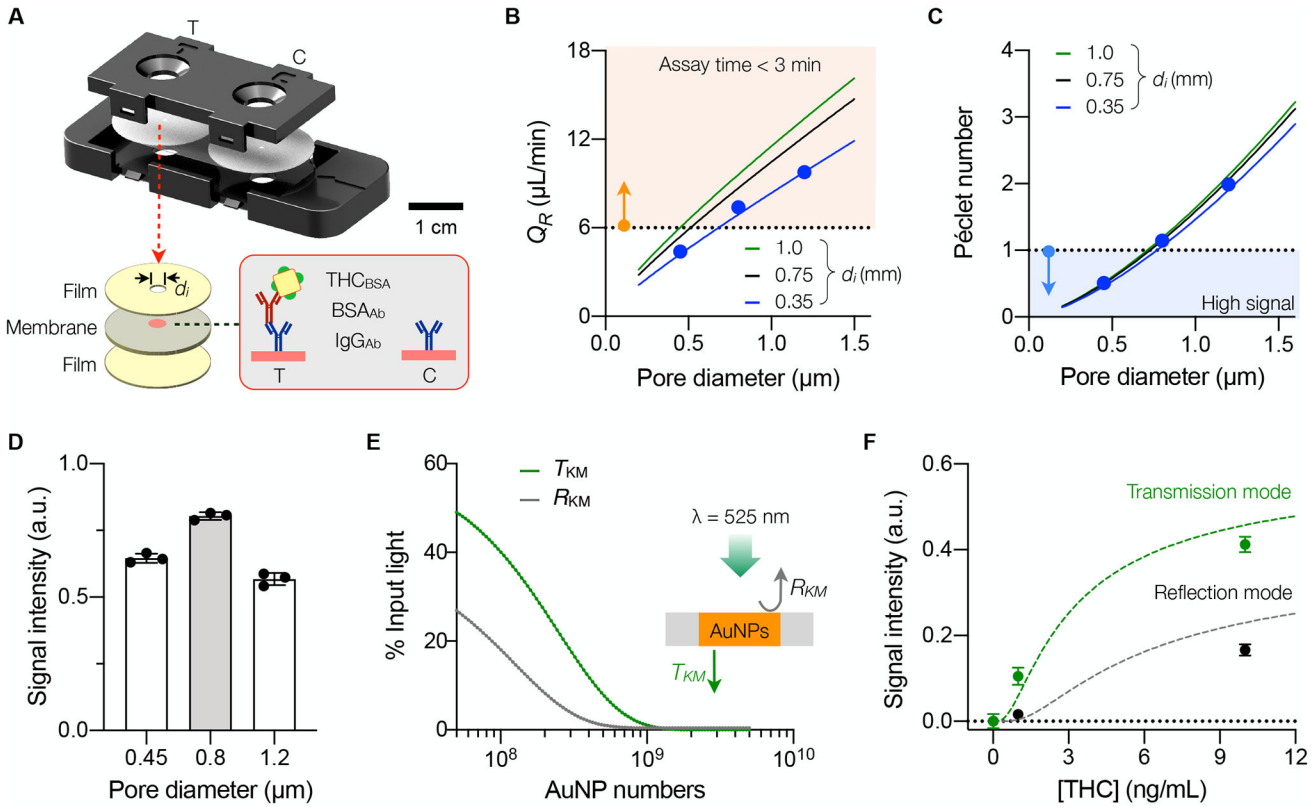

Fig. 3. Engineering the EPOCH membrane sensor.

(A) Schematic of a cartridge. Two sensors, one for the loading control (C) and the other for THC quantification (T), are assembled into a cartridge. Each sensor consists of a radial membrane laminated with plastic films. The small inlet (diameter, d_i) confines samples to pass through the region (red circle) where capture reagents are immobilized. **(B)** Flow rate (Q_R) in a radial sensor as a function of the membrane-pore diameter (d_p). The solid lines are from fluidic modeling, and solid dots from experimental observations (mean ± SD from quadruplicate measurements). The orange-shaded region indicates the required Q_R (>6 μL/min) to meet the assay time of <3 min. **(C)** Péclet number of AuNP$_{Ab}$ inside the membrane sensor. The blue-shaded region indicates low P_e (<1). Solid dots are from experimental data (mean ± SD from quadruplicates). **(D)** Membrane sensors with different d_p. were configured (d_i = 0.35 mm) to capture AuNP$_{Ab}$, and optical signal was compared. Data are shown as mean ± SD from quadruple measurements. **(E)** EPOCH signal from two detection modes (reflection and transmission) was simulated according to the Kubelka–Munk (KM) theory. Under the 525-nm illumination, light transmittance (T_{KM}) is higher than reflectance (R_{KM}). **(F)** Comparison of signal intensities from the transmission and reflection modes. The input samples contained varying amounts of THC mixed with AuNP$_{Ab}$. The transmission mode produced higher analytical signals. Solid dots represent mean ± SD from technical triplicates; dashed lines are from KM simulation.

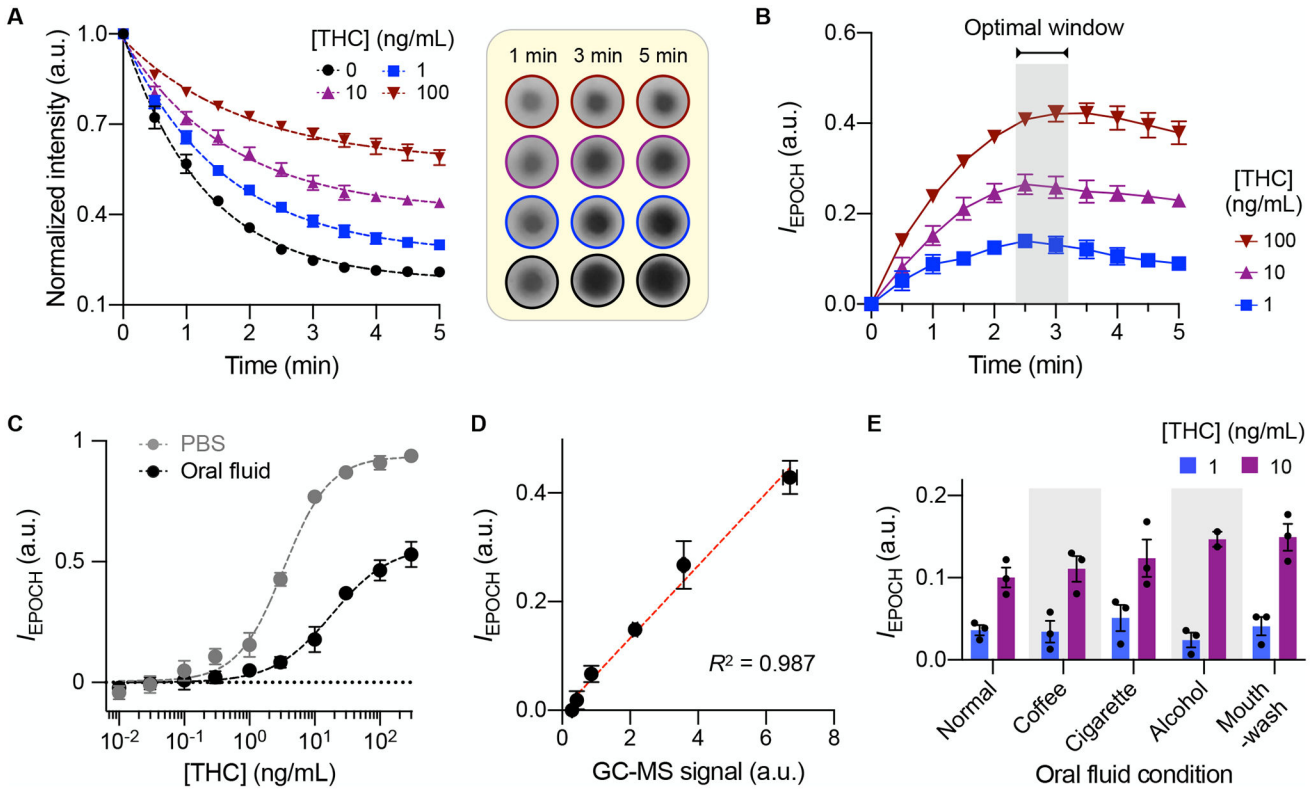

Fig. 4. EPOCH assay characterization.

(A) Temporal signal changes measured at different THC concentrations. The assay followed first-order Langmuir kinetics. The inset (right) shows raw images of $AuNP_{Ab}$ binging spots. **(B)** Net signal differences between THC-positive and control (no THC) samples. **(C)** EPOCH measurements with THC spiked in phosphate-buffered saline (PBS) buffer or oral fluid. The limits of detection were 0.12 (in PBS) and 0.17 (in oral fluid) ng/mL, and the dynamic ranges spanned about 4 orders of magnitude. **(D)** EPOCH results were compared with gas chromatography-mass spectrometry (GC-MS) and found to match well (R^2 = 0.987). **(E)** EPOCH measurements with oral fluid samples collected after activities that affect the oral cavity environment: consuming coffee, smoking cigarettes, drinking beer, and rinsing with mouthwash. Even at [THC] = 1 ng/mL, the signal was significantly higher than background in all oral fluid types (P = 0.0005, one-sided t-test). All data were obtained from technical triplicate measurements and are displayed as mean ± SD.

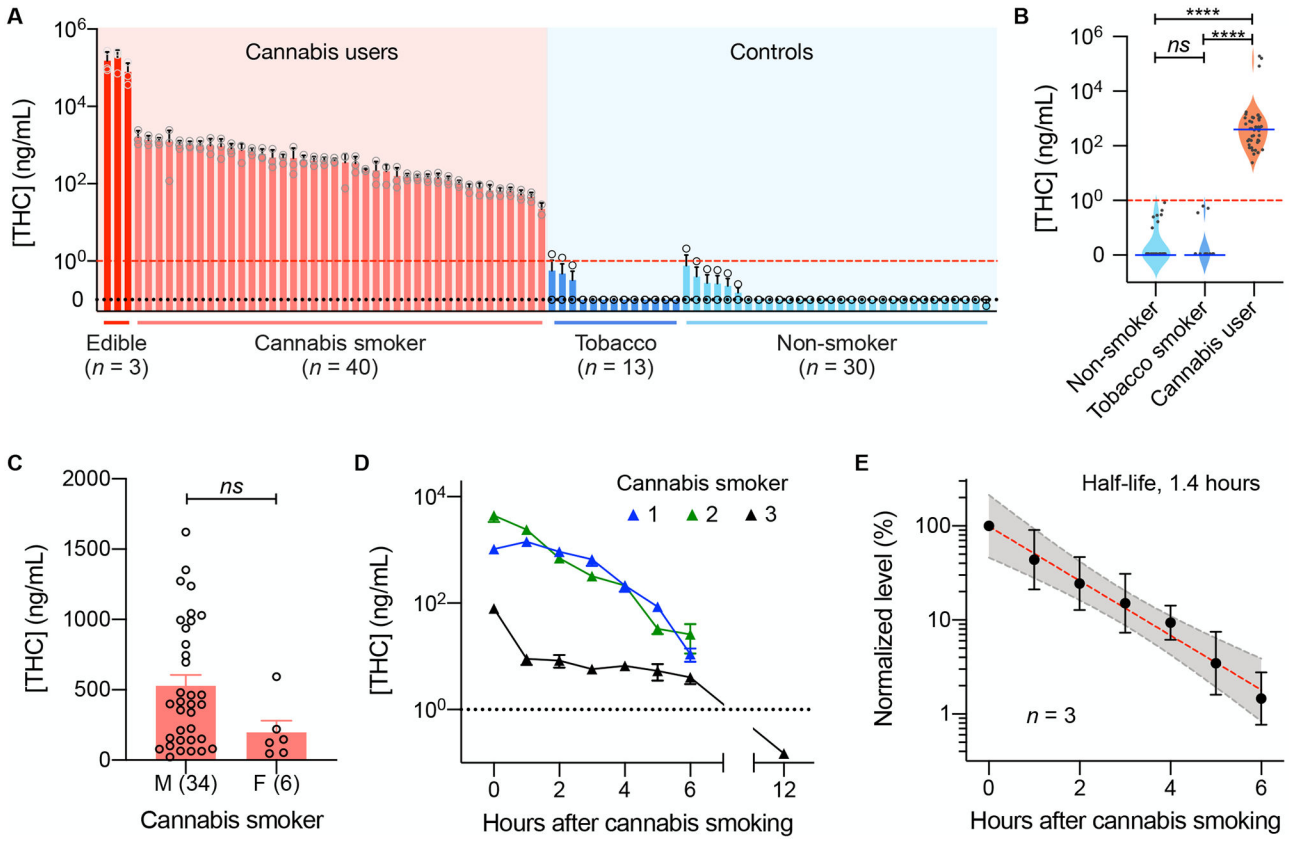

Fig. 5. In-field EPOCH tests of oral fluid samples.

(A) The waterfall plot shows THC concentrations in oral fluid samples from 43 cannabis users (40 cannabis smokers and three THC-infused jelly consumers) and 43 volunteers with no history of cannabis use (13 tobacco smokers and 30 non-smokers). All cannabis-user samples showed high THC concentration above the regulatory guideline (1 ng/mL [THC]). Data are displayed as mean ± SD from triplicate measurements. **(B)** The oral THC concentration was significantly higher in cannabis users than in controls (****$P <$ 0.001, Dunn's multiple comparison test). *ns*, non-significant. **(C)** Between male (M) and female (F) cannabis smokers, the oral THC concentrations showed no significant difference ($P = 0.086$; two-sided t-test). Each data point represents a mean value from triplicate measurements. **(D)** Oral fluid samples from three cannabis users were serially monitored. THC concentrations decreased over time and were expected to fall below the DRUID threshold (dotted line) within 12 hours of cannabis smoking. **(E)** Temporal changes in THC concentrations displayed a single-phase exponential decay ($R^2 = 0.995$) with a half-life of 1.4 hours. The shaded area indicates a 95% confidence band. THC concentrations were normalized against the initial value for each user. Data from three users are displayed as mean ± SD.